

Nanoscopic processes of Current Induced Switching in thin tunnel junctions

J. Ventura, J. P. Araújo, J. B. Sousa, Y. Liu, Z. Zhang and P. P. Freitas, *Member, IEEE*

Abstract—In magnetic nanostructures one usually uses a magnetic field to commute between two resistance (R) states. A less common but technologically more interesting alternative to achieve R-switching is to use an electrical current, preferably of low intensity. Such Current Induced Switching (CIS) was recently observed in thin magnetic tunnel junctions, and attributed to electromigration of atoms into/out of the insulator. Here we study the Current Induced Switching, electrical resistance, and magnetoresistance of thin MnIr/CoFe/AIO_x/CoFe tunnel junctions. The CIS effect at room temperature amounts to 6.9% R-change between the high and low states and is attributed to nanostructural rearrangements of metallic ions in the electrode/barrier interfaces. After switching to the low R-state some electro-migrated ions return to their initial sites through two different energy channels. A low (high) energy barrier of ~0.13 eV (~0.85 eV) was estimated. Ionic electromigration then occurs through two microscopic processes associated with different types of ions sites/defects. Measurements under an external magnetic field showed an additional intermediate R-state due to the simultaneous conjugation of the MR (magnetic) and CIS (structural) effects.

Index Terms—Current Induced Switching, Tunnel Junction, Electromigration, Temperature Dependence, Spin Torque.

I. INTRODUCTION

MAGNETIC tunnel junctions (MTJs) consisting of two ferromagnetic (FM) layers separated by an insulator [1] are strong candidates for technological applications as non-volatile magnetic random-access memories (MRAMs) [2]. The magnetization of one of the FM layers (pinned layer) is fixed by an underlying antiferromagnetic (AFM) layer [3], but the magnetization of the other FM layer (free layer) reverses almost freely when a small magnetic field is applied. Due to spin dependent tunneling [4] one can have two distinct resistance (R) states (the 0 and 1 bits of a magnetic memory), associated with parallel (R_P ; low R) or antiparallel (R_{AP} ; high R) pinned/free layers magnetizations. However, several drawbacks are still of concern for actual MRAM devices, like cross-talk in the array configuration and large power consumption, mainly to generate the magnetic field used to

commute R. It is thus desirable to replace the usual magnetic field-driven by an electrical current-driven resistance switching mechanism. One such mechanism was predicted by Slonczewski and Berger [5], [6] and further developed by others [7], [8] whose studies showed that a spin polarized current can reverse the magnetization of a FM layer by the spin transfer effect, as recently observed in nanometer-sized pillars and exchange-biased spin valves [9], [10], for high current densities ($j \sim 10^8$ A/cm²). On the other hand, Liu et al. [11] observed R-changes induced by much lower current densities ($j \sim 10^6$ A/cm²) in thin tunnel junctions, which did not depend on the relative magnetization orientation in the FM layers. This new effect was called Current Induced Switching (CIS) and attributed to electromigration in nanoconstrictions in the insulating barrier [12]. The underlying physical details are still poorly understood, though their knowledge can be crucial to improve device reliability [13]. One notices that the CIS and spin transfer [14], [15] effects are likely to coexist in thin MTJs for $j \gtrsim 10^6$ A/cm². The reasons for the observed dominance of one effect over the other are still unclear but likely related to structural differences in the studied TJs.

Here we report a study on the transport properties (electrical resistance, magnetoresistance and current induced switching) of thin MnIr/CoFe/AIO_x/CoFe tunnel junctions. Current Induced Switching at room temperature showed a 6.9% resistance change, and the effect is here discussed in terms of nanostructural rearrangements of metallic ions from the FM electrodes near the interface with the insulating barrier. Such rearrangements are mainly reversible and it is remarkable that more than 10^4 R-switching events can be current-induced without significant damage to the tunnel junction.

Two different electromigration energy barrier channels are observed ($\Delta_1 \sim 0.13$ eV; $\Delta_2 \sim 0.85$ eV), associated with ion electromigration between different types of sites/defects near the metal/insulator interfaces, as well as to the lattice binding energies of such ions. The CIS magnitude decreases with decreasing temperature (e.g. 3.5% at $T = 120$ K) showing that the electromigration effect is temperature assisted. Important differences were observed in the CIS cycles when measured under a constant external magnetic field H . In particular, one is able to current-reverse the sign of the exchange bias between the AFM and FM pinned layer, using an adequate current intensity. The effect is due to local heating in narrow nanoconstrictions within the oxide barrier, raising the local temperature above the blocking temperature of the AFM layer. Thus, in addition to the commonly observed two R-states, we can obtain a new intermediate R-state, conjugating the nanostructural and magnetic changes associated respectively

Work supported in part by POCTI/CTM/59318/2004, IST-2001-37334 NEXT MRAM and POCTI/CTM/36489/2000 projects. J. Ventura, Z. Zhang and Y. Liu are thankful for FCT grants (SFRH/BD/7028/2001, SFRH/BPD/1520/2000 and SFRH/BPD/9942/2002).

J. Ventura (e-mail: jventura@fc.up.pt), J. P. Araújo (e-mail: jearaujo@fc.up.pt) and J. B. Sousa (e-mail: jbsousa@fc.up.pt) are with IFIMUP and Physics Department, Faculty of Sciences of University of Porto, R. Campo Alegre, 678, 4169-007, Porto, Portugal.

Y. Liu and Z. Zhang are with INESC Microsystems and Nanotechnologies, R. Alves Redol 9, 1000-029 Lisbon, Portugal.

P. P. Freitas (e-mail: pfreitas@inesc-mn.pt) is with INESC Microsystems and Nanotechnologies and also with Instituto Superior Tecnico, Physics Department, Av. Rovisco Pais, 1000 Lisbon, Portugal.

with the CIS and magnetoresistive (MR) effects.

II. EXPERIMENTAL DETAILS

The complete structure of the Ion Beam Deposited tunnel junction series [11] used in this work is glass/bottom lead/Ta (90 Å)/NiFe (50 Å)/MnIr (90 Å)/CoFe (80 Å)/AlO_x (3 Å+ 4 Å)/CoFe (30 Å)/NiFe (40 Å)/Ta (30 Å)/TiW(N) (150 Å)/top lead. The AlO_x barrier was formed by two-step deposition and oxidation processes. NiFe, CoFe, MnIr and TiW(N) stand for Ni₈₀Fe₂₀, Co₈₀Fe₂₀ and Mn₇₈Ir₂₂, Ti₁₀W₉₀(N). The bottom and top leads are made of Al 98.5% Si 1% Cu 0.5%, 600 Å and 3000 Å thick respectively, and are 26 μm and 10 μm wide. The junctions were patterned to a rectangular shape with areas (A) ranging from 1 × 1 μm² to 4 × 2 μm² by a self-aligned microfabrication process. The samples were annealed at 550 K under an external magnetic field to impress an exchange bias direction between the AFM and FM pinned layers, taken here as the positive direction.

The electrical resistance, magnetoresistance and current induced switching were measured with a four-point d.c. method and an automatic control and data acquisition system. Temperature dependent measurements were performed in a closed cycle cryostat down to 25 K. The CIS cycles were performed using the pulsed current method [16]: current pulses (I_p) of 1 s duration and 5 s repetition period are applied to the TJ, starting with increasingly negative pulses from $I_p = 0$ (junction resistance $\equiv R_{\text{initial}}$), in $\Delta I_p = 2$ or 3 mA steps until a negative maximum $-I_{\text{max}}$ is reached. One then positively increases the current pulses (with the same ΔI_p), following the reverse trend through zero current pulse (R_{half}) up to positive $+I_{\text{max}}$, and then again to zero (R_{final}), to close the CIS hysteretic cycle. The junction *remnant* resistance is always measured in the 5 s-waiting periods between consecutive current pulses, using a low current of 1 mA, thus providing a $R(I_p)$ curve for each CIS cycle. This low-current method allows us to discard non-linear $I(V)$ contributions to the resistance. Positive electrical current is here considered as flowing from the bottom to the top lead.

One then defines the CIS coefficient,

$$CIS = \frac{R_{\text{initial}} - R_{\text{half}}}{(R_{\text{initial}} + R_{\text{half}})/2}, \quad (1)$$

and the resistance shift (δ) in each cycle:

$$\delta = \frac{R_{\text{final}} - R_{\text{initial}}}{(R_{\text{initial}} + R_{\text{final}})/2}. \quad (2)$$

The Tunnel Magnetoresistance is defined as

$$TMR = \frac{R_{\text{AP}} - R_{\text{P}}}{R_{\text{P}}}. \quad (3)$$

III. EXPERIMENTAL RESULTS AND DISCUSSION

A. Electrical resistance and CIS effect

The temperature dependence (300 – 25 K) of the electrical resistance of the studied tunnel junction ($R_{300\text{K}} \approx 5.5 \Omega$; $R \times A \approx 11 \Omega \mu\text{m}^2$ and $TMR = 16\%$) showed a slight quasi-linear R-increase with decreasing temperature, indicating a tunnel-dominated behavior ($dR/dT < 0$), although the presence

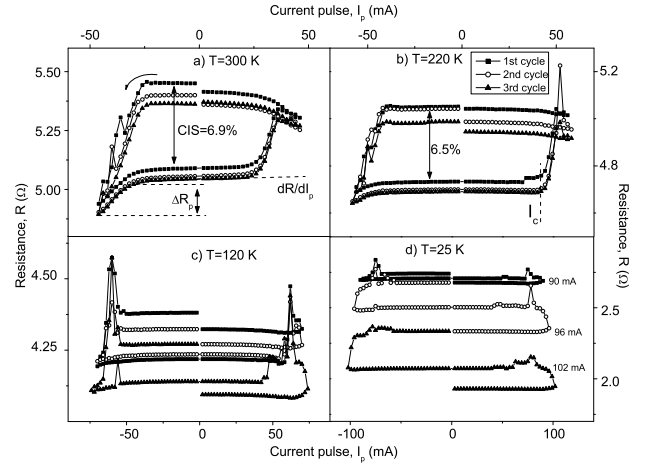


Fig. 1. Current Induced Switching cycles at selected temperatures (300 – 25 K). After each current pulse I_p , the electrical resistance of the tunnel junction is measured under a low bias current (1 mA). R-switching due to electromigration of ions from the electrodes into the barrier is observed for $I_p < -I_c$. For $I_p > I_c$ ions return to the electrodes and a resistance increase is observed. At low temperatures the resistance irreversibly decreases for sufficiently high positive and negative current pulses.

of few or small pinholes cannot be excluded [17]. Measured $I(V)$ characteristics (at room temperature) were fitted using Simmons' model [18] giving a barrier thickness $t = 8.3 \text{ \AA}$ and a barrier height $\varphi = 0.7 \text{ eV}$ (not shown).

We also performed CIS cycles as a function of temperature in the 300 – 25 K range, at $\sim 20 \text{ K}$ intervals, obtaining the results shown in Fig. 1, for some representative curves. Between such CIS cycles measured at different temperatures, $R(T)$ was continuously monitored and a negative dR/dT slope was observed.

Figure 1a) displays three consecutive CIS cycles measured at $T = 300 \text{ K}$ and using $I_{\text{max}} = 46 \text{ mA}$. When increasingly negative current pulses (starting from $I_p = 0$) are applied, one sees that the TJ resistance remains fairly constant (*high R-state*) down to $I_p \approx -24 \text{ mA}$ (where we define the critical switching current, I_c). At this stage, further negative increase in pulse intensity, to $-I_{\text{max}} = -46 \text{ mA}$, produces a sharp resistance decrease ($CIS = 6.9\%$), i.e. switching to a *low R-state*. This indicates a weakening of the oxide barrier, here associated with the migration of ions from the metallic electrodes into the insulator, assisted both by intense electrical fields and local thermal effects. Notice that even a small barrier weakening due to such migration (Fig. 2) could considerably lower the tunnel resistance due to its exponential dependence on barrier thickness [18]. The estimated electrical field at switching is $E \sim 1.5 \text{ MV/cm}$, considerably smaller than that at dielectric breakdown in thin tunnel junctions ($\sim 5 - 10 \text{ MV/cm}$) [19]. On the other hand, local temperatures inside the TJ can rise above 520 K, as experimentally confirmed below. Such high temperatures (combined with $E \sim 1.5 \text{ MV/cm}$) are known to be capable of removing an atom out of its lattice potential well [20].

Returning to Fig. 1a, one sees that a slight increase of the current pulses from $-I_{\text{max}} = -46 \text{ mA}$ up to $I_p \approx -30 \text{ mA}$ is accompanied by a significant rise in resistance (ΔR_p). This

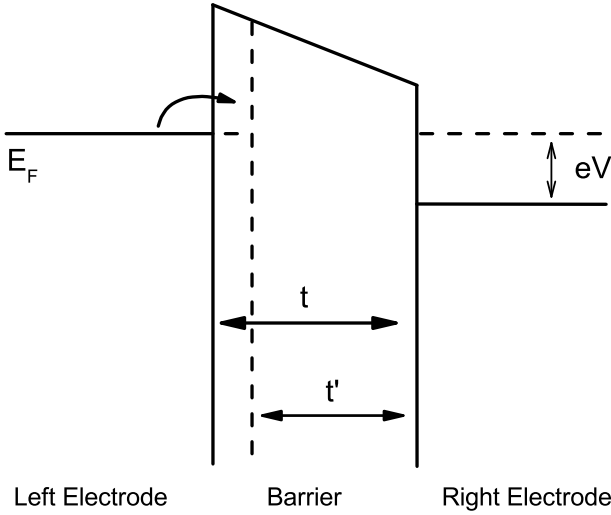


Fig. 2. Electromigration-driven barrier thickness decrease ($t \rightarrow t'$), due to the use of a sufficiently high electrical current across a thin tunnel junction.

indicates that the reduction of the migration driving force (electrical field) allows some atoms to easily return to their initial sites in the metallic electrodes, involving low energy barriers ($\Delta_1 \sim 0.13$ eV). However, most of the displaced ions remain in their local minima inside the oxide barrier since we still have a low R-state. This indicates that the displacement of such ions involves higher energy barriers ($\Delta_2 \sim 0.85$ eV; see below).

Only when the current pulse reaches a sufficiently high positive value ($I_p \approx +24$ mA) does electromigration start in the reverse sense (previously displaced metal ions now move from the oxide into the electrodes), increasing the effective oxide barrier and the TJ electrical resistance. Further increase in I_p produces a small resistance maximum around $+36$ mA. If one reduces the positive pulses from $+I_{\max} = 46$ mA to zero, the plateau of high constant resistance again emerges (R_{final}) below $I_p \simeq 24$ mA. The small difference between R_{final} and R_{initial} indicates a weak irreversibility, i.e. incomplete tunnel junction recovery.

A slightly lower CIS effect of 6.5% (Fig. 1b) is observed at $T = 220$ K. A higher I_{\max} value (58 mA) is used to achieve R-switching, confirming that the CIS effect is thermally activated. An interesting feature develops near $+I_{\max}$ (just after R-switching) leading to a sharp resistance maximum (R_{\max}). This effect gets more enhanced in the second CIS cycle, giving an over-resistive state ($R_{\max} > R_{\text{initial}}$) before declining to the final resistance.

Notice that R-switching is asymmetric with respect to the applied current direction. If one starts a CIS cycle with increasingly positive current pulses, no switching occurs, indicating that only ions from one electrode/barrier interface are active in electromigration [21]. This asymmetry may arise from the fact that the top electrode is deposited over an oxidized *smooth* surface, while a much more irregular bottom electrode/oxide interface is experimentally observed [22]. Since migration of ions into and out of the barrier should occur preferentially in localized nanoconstrictions (where the

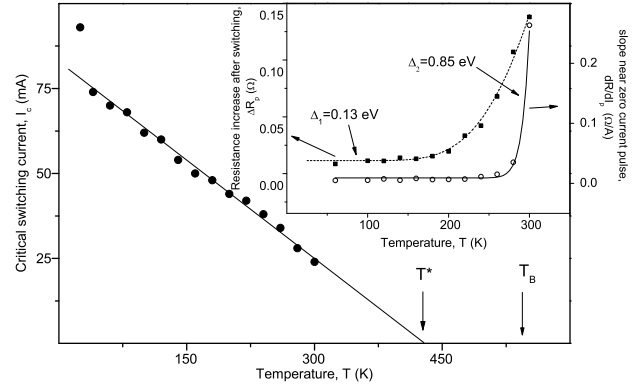


Fig. 3. Temperature dependence of the critical current I_c needed to induce resistance switching, extrapolating to zero at $T^* \approx 425$ K. Inset: temperature dependence of the resistance recovery observed after switching (near $-I_{\max}$; ΔR_p) and of the dR/dI_p slope near zero current pulse.

electrical fields are higher), one concludes that such ions likely belong to the bottom electrode. In fact, the Current Induced Switching effect is strongly dependent on the topography of the electrode/barrier interface as experimentally observed in magnetic tunnel junctions with different barrier thicknesses and different insulating barrier materials [12].

Measurements performed at $T = 120$ K give considerably lower CIS signals ($\sim 3.5\%$; Fig. 1c), again requiring higher I_{\max} (70 mA) for switching. In addition to the previously observed anomalous resistance maximum near $+I_{\max}$, a similar effect also arises near $-I_{\max}$, again giving an over-resistive state. In the third CIS cycle (under $I_{\max} = 74$ mA), the resistance suddenly irreversibly decreases when $I_p \gtrsim +70$ mA. This low R-value persists with the subsequent decrease of I_p to zero. Thus, sufficiently high I_p values cause irreversible oxide-barrier degradation.

To ensure resistance switching at $T = 25$ K (Fig. 1d) we adopted $I_{\max} = 90$ mA in the first cycle. The anomalous resistance maxima near $\pm I_{\max}$ are now much attenuated but the resistance systematically shows collapsing steps (irreversible junction degradation) both at positive and negative high current pulses. Subsequent $R(T)$ measurements indicate metallic conductance in the TJ ($dR/dT > 0$). This means that metallic-like paths are opened across the insulating barrier (formation or enlargement of pinholes) while performing CIS cycles under high I_{\max} values and now dominate the tunnel junction conductance.

The temperature dependence of the critical current needed to induce resistance switching (I_c ; see Fig. 1b) was found to exhibit a quasi-linear decrease with increasing temperature, extrapolating to zero at $T^* \approx 425$ K, as shown in Fig. 3. Such behavior can be understood if one considers the expression for the effective barrier modified by electromigration [23] $E_0 - \xi I$, where E_0 is the zero-bias electromigration-energy barrier, ξ is a parameter that measures the change of such activation energy as a result of the electromigration force [24] and I is the applied current. Electromigration then occurs when the effective barrier becomes comparable to the thermal energy. The temperature dependence of the critical current (I_c) is then

given by [25]:

$$I_c \approx \frac{E_0}{\xi} - \frac{k_B T}{\xi}, \quad (4)$$

where k_B is the Boltzmann constant. Although our data could be well fitted using this simple model, one should notice that the effective temperature inside the tunnel junctions is larger than that at which the measurement takes place (see below), which limits the quantitative understanding of our results.

On the other hand, the localized resistance increase (ΔR_p) observed just after switching at high negative current pulses (see Fig. 1) shows an exponential temperature dependence $e^{-\Delta_1/k_B T}$ with $\Delta_1 \approx 0.13$ eV (inset of Fig. 3). This is attributed to local low barrier channels for atomic migration of displaced metal ions, from the barrier into the electrode. Additionally, the slope of the CIS cycles near $I_p = 0$ (in the low R-branch; dR/dI_p in Fig. 1a), gives an indication on the remaining high energy barriers, with $\Delta_2 \approx 0.85$ eV. This value is fairly close to the activation energy for atomic diffusion through grain boundaries in CoFe/Cu multilayers (0.90 eV) [26]. One concludes that ionic electromigration can occur through two microscopic processes with different energy barriers. These channels may be associated with electromigration of ions with different binding energies (and migration energies [27]), or trapped at deep potential sites in the oxide lattice and/or at oxygen vacancies [28], [29].

We also studied the influence of the current pulse duration and current cycling on the CIS effect. The critical switching current I_c (CIS coefficient) increases (decreases) with shortening pulse time (down to ns). The CIS coefficient under ns pulses can be improved by heating the sample up to 400 K. The best results achieved in these type of structures correspond to a critical switching current density of 2×10^6 A/cm² for 10-ns pulses, leading to a CIS coefficient of 3.8%. With regard to current cycling, two effects are observed: first, a temperature increase leads to a reversible resistance decrease. Then, small irreversible barrier damage occurs due to the irreversible creation and/or enlargement of nanoconstrictions and pinholes. For measurements up to 10^4 cycles (using ms-pulses), a stable junction resistance (indicative of barrier stability) is achieved after the first 6000 pulses. Once this "equilibrium" resistance is reached for a certain temperature and current pulse, one can, in principle, apply much larger pulse numbers.

B. CIS effect under an external magnetic field

A new junction from the same series ($R_{300K} \approx 8 \Omega$; $R \times A \approx 48 \Omega \mu\text{m}^2$) was used to study the influence of the magnetic field on the CIS effect. Figure 4 displays the initial sets of consecutive MR(H) and CIS (R vs. I_p) measurements at room temperature. The CIS cycles were performed under constant magnetic field of 0 and ± 200 Oe, and with $I_{\text{max}} = 39$ mA.

The MR(H) cycle displayed in Fig. 4a-1 ($TMR = 14\%$) shows the usual low (high) R-state associated with parallel (\Rightarrow antiparallel; \Leftarrow) free/pinned layers magnetizations. The following CIS cycle was measured with $H = -200$ Oe (Fig. 4b-1), thus starting in the \Leftarrow high R-state. One again observes resistance switching to a low R-state for $I_p \lesssim -21$ mA (CIS = 15%; notice the different denominators in the TMR

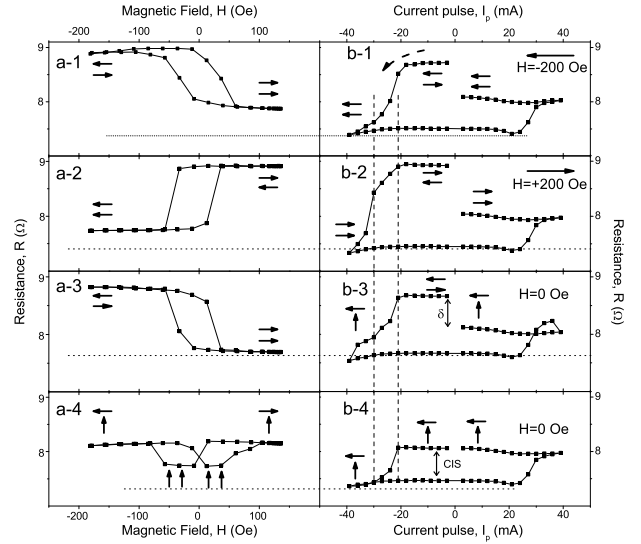


Fig. 4. Magnetoresistance (left column) and subsequent Current Induced Switching cycles (right column) measured under an external magnetic field. Notice the inversion of the MR(H) behavior after CIS cycles performed under an applied magnetic field opposite to the exchange bias. Pairs of arrows represent the magnetizations of the pinned (bottom arrow) and free layer (top arrow), defining different TJ magnetic states. \uparrow denotes a domain state.

and CIS definitions). The final R-value attained at $-I_{\text{max}}$ is lower than the parallel state resistance R_P of the precedent MR(H) cycle (Fig. 4a-1). Thus, the observed R-switching cannot be due to a magnetoresistive effect only, but should also have a structural contribution.

To clarify the precedent remark one first notices that the subsequent MR cycle (Fig. 4a-2) appears *inverted* with respect to that of Fig. 4a-1. This means that in the previous CIS cycle under $H = -200$ Oe (Fig. 4b-1) a change in the sign of the exchange bias has occurred. This effect is attributed to localized heating in nanoconstrictions in the barrier, under high current pulses, rising the temperature above the blocking temperature of the MnIr AFM layer ($T_B = 520$ K; [30]). The magnetization of the pinned layer is then free to align with the applied magnetic field (\mathbf{H} opposite to the initial exchange bias), impressing, upon cooling below T_B , a new (inverted) exchange bias. The junction magnetic state has then switched from antiparallel (\Leftarrow) to parallel (\Rightarrow) through the reversal of the pinned layer. The difference between the low R-state (observed near $-I_{\text{max}}$) and R_P is then due to electromigration of metallic ions from the electrodes into the barrier.

Thermally assisted electromigration in the opposite direction (increasing R) occurs only for $I_p \gtrsim 21$ mA. At the end of the CIS cycle the junction is in the parallel \Rightarrow state and a large difference between R_{initial} and R_{final} ($\delta = -7\%$) is observed, leading to an *intermediate* R-state.

Although the MR(H) cycle of Fig. 4a-2 is inverted relatively to that of Fig. 4a-1, the TMR coefficient remains practically unchanged. The following CIS measurement was performed under a positive field $H = +200$ Oe (Fig. 4b-2), giving a CIS coefficient of 18% and $\delta = -10\%$ (again an intermediate state).

The third MR(H) cycle (Fig. 4a-3) was similar to the

initial one (Fig. 4a-1), indicating that the CIS cycle under $H = +200$ Oe (Fig. 4b-2) reverted the sample into its original magnetic state (parallel \Rightarrow state; the newly induced exchange bias direction is that impressed during deposition). Subsequent CIS measurements *without a magnetic field* lead to $CIS = 12\%$ and $\delta = -7\%$ (Fig. 4b-3). Notice that when the temperature rises above T_B the pinned layer magnetization (under $H = 0$) develops a complex multi-domain structure (Fig. 4b-3, see arrows; \uparrow denotes a domain-like state). Accordingly, the following MR measurement (Fig. 4a-4) shows a double MR loop with a considerably lower TMR (5%) due to the lack of full parallelism between the free and pinned layer magnetizations. Finally, in the subsequent CIS cycle (Fig. 4a-4), measured under *zero magnetic field*, one has $R_{\text{final}} \approx R_{\text{initial}}$ (resistance shift $\delta = -0.04\%$) and $CIS = 8\%$. The observed R-switching is now only due to the migration of ions into/out of the barrier (magnetization reversal of the pinned layer does not occur) and the negligible resistance shift is attributed to small barrier degradation. Notice that in both CIS cycles under $H = 0$ and $H \neq 0$, R-switching always occurs at $I_p \approx -21$ mA, indicating that the structural effect precedes the magnetic one (see corresponding vertical lines in Fig. 4, column b).

IV. CONCLUSIONS

In conclusion, we presented a detailed study of the Current Induced Switching effect on low resistance, thin $\text{CoFe}/\text{AlO}_x/\text{CoFe}$ tunnel junctions. We consistently traced the evolution of resistance switching in consecutive CIS cycles between two (or three) states, driven by an electrical current, both under $H = 0$ and $H \neq 0$. Such evolution is controlled by the nanostructural rearrangements of ions at the electrodes/barrier interfaces (electromigration) and also by magnetic switching in the pinned layer under sufficiently high current pulses (under $H \neq 0$).

The CIS measurements as a function of temperature (300 – 25 K) showed that this effect is thermally assisted. Both low (~ 0.13 eV) and high (~ 0.85 eV) energy barriers were estimated and associated with electromigration involving different types of ions sites/defects. At low temperatures one observes irreversible resistance decreases near $\pm I_{\text{max}}$, indicating barrier degradation. If CIS cycles are measured under an external magnetic field, one is able to current-induce a change in the sign of the exchange bias of the TJ, and the corresponding magnetic state (antiparallel to parallel). This effect arises from excessive local heating in the TJ, and enables us to obtain a CIS cycle with three different electrical resistance states.

REFERENCES

- [1] J. S. Moodera, L. R. Kinder, T. M. Wong, and R. Meservey, “Large magnetoresistance at room temperature in ferromagnetic thin film tunnel junctions”, *Phys. Rev. Lett.*, vol. 74, pp. 3273–3276, April 1995.
- [2] B. N. Engel, N. D. Rizzo, J. Janesky, J. M. Slaughter, R. Dave, M. DeHerrera, M. Durlam, and S. Tehrani, “The Science and Technology of Magnetoresistive Tunneling Memory”, *IEEE Trans. Nanotechnol.*, vol. 1, pp. 32–38, March 2002.
- [3] J. Nogués and I. K. Schuller, “Exchange bias”, *J. Magn. Magn. Mater.*, vol. 192, pp. 203–232, February 1999.
- [4] P. M. Tedrow and R. Meservey, “Spin-dependent tunneling into ferromagnetic Nickel”, *Phys. Rev. Lett.*, vol. 26, pp. 192–195, January 1971.
- [5] J. C. Slonczewski, “Current-driven excitation of magnetic multilayers”, *J. Magn. Magn. Mater.*, vol. 159, pp. L1–L7, June 1996.
- [6] L. Berger, “Emission of spin waves by a magnetic multilayer traversed by a current”, *Phys. Rev. B*, vol. 54, pp. 9353–9358, October 1996.
- [7] M. D. Stiles and A. Zangwill, “Anatomy of spin-transfer torque”, *Phys. Rev. B*, vol. 66, no. 1, pp. 014407, June 2002.
- [8] S. Zhang, P. M. Levy, and A. Fert, “Mechanisms of spin-polarized current-driven magnetization switching”, *Phys. Rev. Lett.*, vol. 88, no. 23, pp. 236601, June 2002.
- [9] J. A. Katine, F. J. Albert, R. A. Buhrman, E. B. Myers, and D. C. Ralph, “Current-Driven Magnetization Reversal and Spin-Wave Excitations in Co/Cu/Co Pillars”, *Phys. Rev. Lett.*, vol. 84, pp. 3149–3152, April 2000.
- [10] Y. Jiang, S. Abe, T. Ochiai, T. Nozaki, A. Hirohata, N. Tezuka, and K. Inomata, “Effective reduction of critical current for current-induced magnetization switching by a Ru lLayer insertion in an exchange-biased spin valve”, *Phys. Rev. Lett.*, vol. 92, no. 16, pp. 167204, April 2004.
- [11] Y. Liu, Z. Zhang, P. P. Freitas, and J. L. Martins, “Current-induced magnetization switching in magnetic tunnel junctions”, *Appl. Phys. Lett.*, vol. 82, pp. 2871–2873, April 2003.
- [12] A. Deac, O. Redon, R. C. Sousa, B. Dieny, J. P. Nozières, Z. Zhang, Y. Liu, and P. P. Freitas, “Current driven resistance changes in low resistance x area magnetic tunnel junctions with ultra-thin Al-O_x barriers”, *J. Appl. Phys.*, vol. 95, pp. 6792–6794, June 2004.
- [13] S. Bae, I. F. Tsu, M. Davis, E. S. Murdock, and J. H. Judy, “Electromigration study of magnetic thin films for the electrical reliability of spin valves read heads”, *IEEE Trans. Magn.*, vol. 38, pp. 2655–2657, September 2002.
- [14] Y. Huai, F. Albert, P. Nguyen, M. Pakala, and T. Valet, “Observation of spin-transfer switching in deep submicron-sized and low-resistance magnetic tunnel junctions”, *Appl. Phys. Lett.*, vol. 84, pp. 3118–3120, April 2004.
- [15] G. D. Fuchs, N. C. Emley, I. N. Krivorotov, P. M. Braganca, E. M. Ryan, S. I. Kiselev, J. C. Sankey, D. C. Ralph, R. A. Buhrman, and J. A. Katine, “Spin-transfer effects in nanoscale magnetic tunnel junctions”, *Appl. Phys. Lett.*, vol. 85, pp. 1205–1207, August 2004.
- [16] Y. Liu, Z. Zhang, and P. P. Freitas, “Hot-spot mediated current-induced resistance change in magnetic tunnel junctions”, *IEEE Trans. Magn.*, vol. 39, pp. 2833–2835, September 2003.
- [17] B. Oliver, Q. He, X. Tang, and J. Nowak, “Tunneling criteria and breakdown for low resistive magnetic tunnel junctions”, *J. Appl. Phys.*, vol. 94, pp. 1783–1786, August 2003.
- [18] J. G. Simmons, “Generalized formula for the electrical tunnel effect between similar electrodes by a thin insulating films”, *J. Appl. Phys.*, vol. 34, pp. 1793–1803, June 1963.
- [19] B. Oliver, Q. He, X. Tang, and J. Nowak, “Dielectric breakdown in magnetic tunnel junctions having an ultrathin barrier”, *J. Appl. Phys.*, vol. 91, pp. 4348–4352, April 2002.
- [20] Z. Chen and R. S. Sorbello, “Local heating in mesoscopic systems”, *Phys. Rev. B*, vol. 47, pp. 13527–13534, May 1993.
- [21] J. Ventura, J. B. Sousa, Y. Liu, Z. Zhang, and P. P. Freitas, “Electromigration in thin tunnel junctions with ferromagnetic/nonmagnetic: nanoconstrictions, local heating, and direct and wind forces”, *Phys. Rev. B*, vol. 72, pp. 094432, September 2005.
- [22] J. Wang, Y. Liu, P. P. Freitas, E. Snoeck, and J. L. Martins, “Continuous thin barriers for low-resistance spin-dependent tunnel junctions”, *J. Appl. Phys.*, vol. 93, pp. 8367–8369, May 2003.
- [23] K. S. Ralls, D. C. Ralph, and R. A. Buhrman, “Individual-defect electromigration in metal nanobridges”, *Phys. Rev. B*, vol. 40, pp. 11561–11570, December 1989.
- [24] P. A. M. Holweg, J. Caro, A. H. Verbruggen, and S. Radelaar, “Ballistic electron transport and two-level resistance fluctuations in noble-metal nanobridges”, *Phys. Rev. B*, vol. 45, pp. 9311–9319, April 1992.
- [25] H. Yasuda and A. Sakai, “Conductance of atomic-scale gold contacts under high-bias voltages”, *Phys. Rev. B*, vol. 56, pp. 1069–1072, July 1997.
- [26] E. B. Svedberg, K. J. Howard, M. C. Bønsager, B. B. Pant, A. G. Roy, and D. E. Laughlin, “Interdiffusion in CoFe/Cu multilayers and its application to spin-valve structures for data storage”, *J. Appl. Phys.*, vol. 94, pp. 1001–1006, July 2003.
- [27] J. V. Barth, “Transport of adsorbates at metal surfaces: from thermal migration to hot precursors”, *Surf. Sci. Rep.*, vol. 40, pp. 75–149, October 2000.

- [28] J. A. Rodriguez, J. Hrbek, Z. Chang, J. Dvorak, T. Jirsak, and A. Maiti, "Importance of O vacancies in the behavior of oxide surfaces: Adsorption of sulfur on $\text{TiO}_2(110)$ ", *Phys. Rev. B*, vol. 65, no. 23, pp. 235414, June 2002.
- [29] N. Nilius, T. M. Wallis, and W. Ho, "Influence of a Heterogeneous Al_2O_3 Surface on the Electronic Properties of Single Pd Atoms", *Phys. Rev. Lett.*, vol. 90, no. 4, pp. 046808, January 2003.
- [30] H. Li, P. P. Freitas, Z. Wang, J. B. Sousa, P. Gogol, and J. Chapman, "Exchange enhancement and thermal anneal in $\text{Mn}_7\text{Ir}_{24}$ bottom-pinned spin valves", *J. Appl. Phys.*, vol. 89, pp. 6904–6906, June 2001.